Strategies for p-type doping of $ZnGeN_2$

Nicholas L. Adamski[a)]
Department of Electrical and Computer Engineering, University of California, Santa Barbara, CA 93106-9560, USA
Zhen Zhu, Darshana Wickramaratne, and Chris G. Van de Walle
Materials Department, University of California, Santa Barbara, CA 93106-5050, USA

(Dated: 15 May 2019)

$ZnGeN_2$ has been proposed as an attractive semiconductor for a number of applications, but doping is largely unexplored. We examine the behavior of Li, Cu, Al, Ga, In and C as candidate acceptors using hybrid density functional theory. Cu, In, and C give rise to deep acceptor levels, but Li, Al, or Ga could potentially lead to p-type conductivity. Al is particularly attractive, since it has an ionization energy of 0.24 eV, comparable to Mg in GaN. However, self-compensation due to wrong-site incorporation is a serious issue. We demonstrate that co-doping with hydrogen can be used to overcome this problem.

The II-IV-nitride semiconductors are based on earth-abundant elements and have band gaps that span a wide range of energies. $ZnGeN_2$ is a prototype example: it has a direct band gap reported between 2.99 eV and 3.30 eV,[1,2] and this gap can be tuned by alloying with Sn or Si, making it attractive for applications in quantum cascade lasers,[3] multijunction solar cells,[4] and light emitting diodes.[5]

For all of these applications, controlled doping is crucial. n-type doping is usually not a problem in nitride semiconductors,[6,7] but p-type doping has proven challenging in the III-nitrides due to the dearth of acceptor dopants with low ionization energies.[8] The use of Mg to achieve controlled p-type doping has been a big driver for the success of GaN in optoelectronics.[9] Translating this success to the II-IV-nitrides requires a thorough understanding of the electronic properties of candidate p-type dopants. At present, no experimental reports on p-type doping of $ZnGeN_2$ are available. Accurate first-principles calculations can lead the way in addressing the prospects and challenges associated with acceptor doping in $ZnGeN_2$.

Skachkov *et al.*[10] previously performed density functional theory (DFT) calculations on Ga acceptors in $ZnGeN_2$. They used the local density approximation (LDA), which severely underestimates the band gap. They corrected the band gap by applying an on-site potential U, but this approach does not necessarily produce the correct position of the valence-band maximum (VBM).[7,11] The LDA also falls short in describing charge localization, an issue that is particularly important for correctly calculating the ionization energy of acceptors.[12] Use of a hybrid functional overcomes these problems. Hybrid functional calculations were applied by Wang *et al.*[13] to $ZnSnN_2$, which has a lower band gap than $ZnGeN_2$; they identified Li_{Zn} as a shallow acceptor.

In the present work, we investigate p-type doping of $ZnGeN_2$ using a hybrid functional. Acceptor doping of $ZnGeN_2$ can be achieved with group-I elements substituting on the Zn site; group-III elements substituting on the Ge site; or group-IV elements substituting on the N site. We examine a wide array of candidate acceptors: Li_{Zn}, Li_{Ge}, Cu_{Zn}; Al_{Ge}, Ga_{Ge}, and In_{Ge}; and C_N. Among these, Li_{Zn}, Al_{Ge}, and Ga_{Ge} will be found to have small enough ionization energies to enable p-type conductivity.

We also examine compensation by native defects, as well as self-compensation due to incorporation of the dopant on the "wrong" site: for instance, Al_{Ge} acts as an acceptor, but Al_{Zn} as a donor. The similarity in ionic radii between Zn and Ge indeed leads to a propensity for wrong-site substitution, causing severe self-compensation. We will also propose a potential solution in the form of co-doping with hydrogen. The incorporation of hydrogen donors can be more favorable than the incorporation of wrong-site dopants, thus suppressing self-compensation. Our detailed examinations include calculations of hydrogen-dopant complexes, thus providing guidance as to whether codoping with hydrogen and subsequent removal of hydrogen in a post-growth anneal is a viable route for p-type doping in $ZnGeN_2$.

Our DFT calculations are performed with projector augmented wave potentials[14] as implemented in the Vienna *Ab-initio* Simulation Package (VASP).[15,16] We use the hybrid functional of Heyd, Scuseria, and Ernzerhof (HSE)[17,18] with a standard mixing parameter of 25%. Zn $3d^{10}4s^2$, Ge $4s^24p^2$ and N $2s^22p^3$ electrons are treated as valence, and the plane-wave basis cutoff is 400 eV. $ZnGeN_2$ has the orthorhombic $Pna2$ space group; the lattice parameters can be related to wurtzite parameters via $a \approx \sqrt{3}a_w$, $b \approx 2a_w$, and $c = c_w$.[1,19] Note that some authors define the axes with a and b interchanged.[20,21] We calculate the lattice parameters to be a=5.47 Å, b=6.45 Å, and c=5.20 Å, which are within 0.5% of experimental values.[19] Our HSE band gap for $ZnGeN_2$ is 3.19 eV, which lies within the range of the experimentally reported values.[1,2] Defect calculations are performed in a 128-atom supercell with a single special **k** point (1/4, 1/4, 1/4). Spin polarization was included.

For an acceptor A with charge state q the formation

a)Electronic mail: nadamski@ece.ucsb.edu

energy $E^f(A^q)$ is calculated as:[11]

$$E^f(A^q) = E_{\rm tot}(A^q) - E_{\rm tot}({\rm bulk}) + \sum_i n_i\mu_i + qE_F + \Delta^q\,, \quad (1)$$

where $E_{\rm tot}(A^q)$ is the energy of the $ZnGeN_2$ supercell with the acceptor in the charge state q, $E_{\rm tot}({\rm bulk})$ is the energy of the pristine supercell, n_i represents the number of atoms of species i that are added to (n_i<0) or removed from (n_i>0) the supercell, and μ_i is the chemical potential of these atoms. The electronic chemical potential E_F is given by the position of the Fermi level referenced to the valence-band maximum (VBM). Finally, the term Δ^q is the charge-state dependent correction to the formation energy due to the finite size of the supercell.[22,23]

The atomic chemical potentials, μ_i, are variables that reflect the growth conditions; they are constrained by the formation enthalpy of competing phases. For the host elements, our calculations span the range from Zn-rich (Ge-poor) to Zn-poor (Ge-rich) conditions; the region of stability of $ZnGeN_2$ was described in detail in Ref. 7. For our investigations of candidate acceptors, we use Li_3N, Cu metal, diamond, AlN, GaN and InN as limiting phases. For each dopant configuration we report a formation energy based on chemical potentials that would maximize the incorporation of the acceptor on their respective substitutional site, based on calculated formation enthalpies for Li_3N (−1.65 eV), AlN (−3.15 eV), and GaN (−1.2 eV); these values are in agreement with experiment.[24,25] In our calculations involving hydrogen we assume $\mu_{\rm H}$ is determined by the H_2 molecule at T=0.

The ionization energy of an acceptor is given by the thermodynamic charge-state transition level, $\epsilon(q/q')$. This transition level is defined as the Fermi-level position below which the defect is stable in the charge state q and above which it is stable in the charge state q'. For example, for the case of the Al_{Ge} acceptor, the ionization energy is determined as:

$$\epsilon(0/-) = E^f({\rm Al_{Ge}}^{-1}; E_F = 0) - E^f({\rm Al_{Ge}}^{0}; E_F = 0). \quad (2)$$

where $E^f({\rm Al_{Ge}}^{-1}; E_F = 0)$ is the formation energy of Al_{Ge} in the negative charge when the Fermi level is at the VBM and $E^f({\rm Al_{Ge}}^{0}; E_F = 0)$ is the formation energy of Al_{Ge} in the neutral charge state.

The calculated charge-state transition levels are shown in Fig. 1. From this figure it is clear that Cu_{Zn}, In_{Ge}, and C_N have deep acceptor levels and cannot lead to p-type conductivity in $ZnGeN_2$. We also considered Li_{Ge} and find it has a large ionization energy (1.01 eV). The best candidates for shallow acceptors are Li_{Zn}, Al_{Ge} and Ga_{Ge}, with ionization energies of 0.36, 0.24, and 0.30 eV, as listed in Table I. The ionization energy of Al_{Ge}, 0.24 eV, is close to the ionization energy for Mg_{Ga} in GaN (0.26 eV, Ref. 8) and would thus lead to a reasonable hole concentration. The equations for carrier concentrations in a doped semiconductor show that the hole concentration at room temperature decreases by roughly an order of magnitude for every 100 meV increase in ionization energy. An ionization energy of 0.46 eV due to In_{Ge} would therefore probably be too high to lead to a useful hole concentration. Hence, among the acceptors we have investigated, p-type doping of $ZnGeN_2$ should be feasible using Li, Al, or Ga.

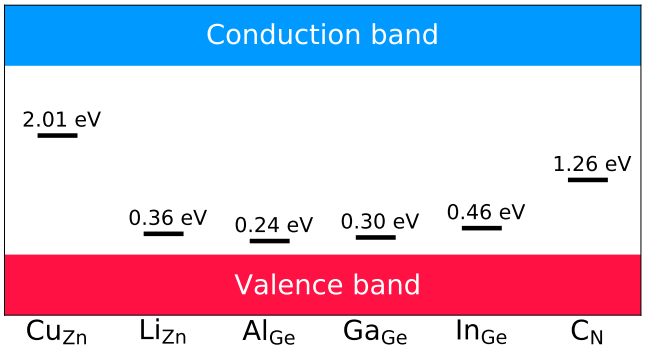

FIG. 1. Thermodynamic transition levels for candidate acceptors in $ZnGeN_2$. The zero of energy is set at the VBM. Values for ionization energies are indicated.

TABLE I. Properties of candidate acceptors in $ZnGeN_2$. $\epsilon(0/-)$ is the acceptor level referenced to the VBM (i.e., the ionization energy). $E_b(A$–$D)$ is the binding energy of the acceptor-donor complex, where the donor is the dopant incorporated on the wrong site. $E_b(A$–H) the binding energy of the acceptor-hydrogen complex. All quantities are in eV.

	Li_{Zn}	Al_{Ge}	Ga_{Ge}
$\epsilon(0/-)$	0.36	0.24	0.30
$E_b(A$–$D)$	0.99	0.57	0.58
$E_b(A$–H)	1.08	0.55	0.58

We now discuss the atomic structure of these potential p-type dopants. In Fig. 2(d)-(i), we illustrate the local relaxations in terms of deviations from the bulk bond lengths. For Li_{Zn} in the negative charge state [Fig. 2(e)], a small breathing relaxation occurs in which the Li-N bonds are extended by ∼1% compared to Zn-N bond lengths in the bulk. In the neutral charge state, however, a large asymmetric relaxation occurs [Fig. 2(d)]: three Li-N bonds contract by ∼1.6%, while the fourth Li-N bond extends by 16%, compared to the bulk Zn-N bond lengths. For Al_{Ge}^{-} [Fig. 2(g)], there is a breathing relaxation in which Al-N bonds extend by ∼0.4% of the bulk Ge-N bond length; for Ga_{Ge}^{-} [Fig. 2(i)], this relaxation is an extension of Ga-N bonds by ∼3.7%. The smaller relaxation of the N atoms in the case of Al_{Ge} compared to Ga_{Ge} can be understood by comparing the ionic radii of Al and Ga in the 3+ charge state with Ge in the 4+ charge state: the ionic radius of Al is identical to that of Ge (0.39 Å), while that of Ga is significantly larger (0.47 Å).[26] In the neutral charge state, Al_{Ge} [Fig. 2(f)] and Ga_{Ge} [Fig. 2(h)] exhibit an asymmetric relaxation. For Al_{Ge}, one of the Al-N bond lengths is 2.7% longer than bulk Ge-N bonds, while the other three Al-N bonds

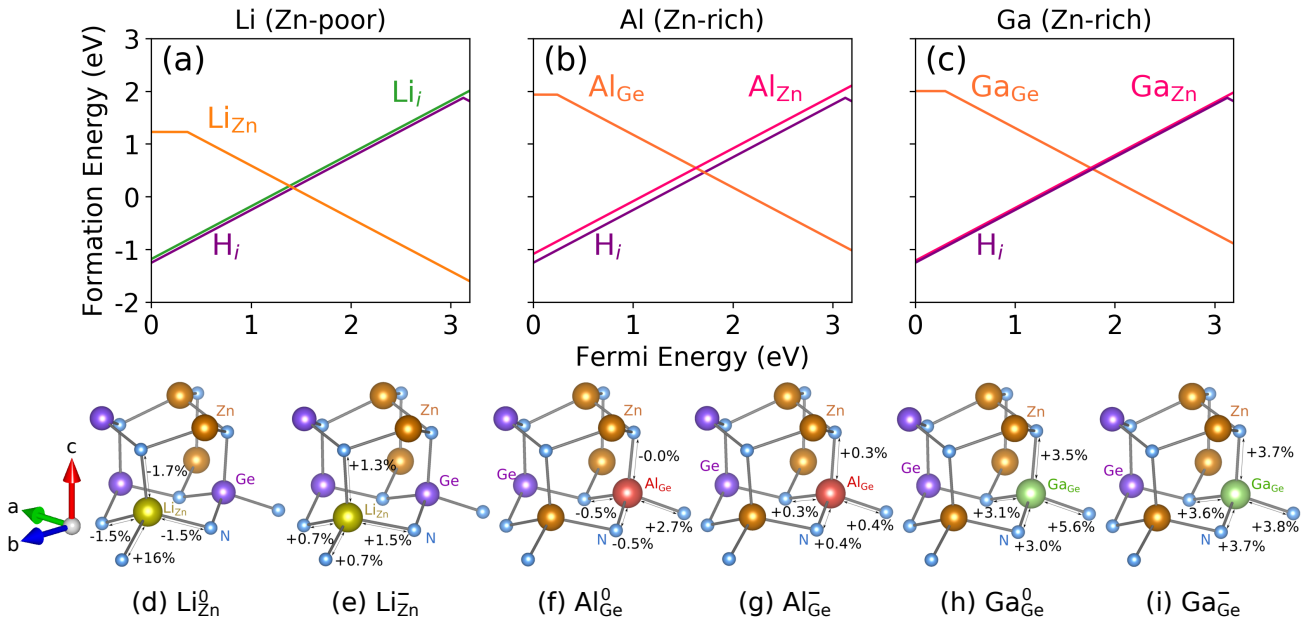

FIG. 2. Formation energies for (a) Li, (b) Al and (c) Ga in $ZnGeN_2$. The chemical-potential conditions used in each case are shown at the top of each panel. Local relaxations for (d), (e) Li_{Zn}, (f), (g) Al_{Ge}, and (h), (i) Ga_{Ge} in the neutral and negative charge states.

are close to the bulk Ge-N bond lengths. For Ga_{Ge}, one of the Ga-N bond lengths is 5.6% longer than the bulk Ge-N bond lengths, while the other three bonds are only about 3.1% longer than bulk lengths.

The formation energies of these candidate acceptors are illustrated in Fig. 2(a)-(c). In each case, we focus on a regime where incorporation of the appropriate substitutional configuration of the acceptor is favored: Li should go on a Zn site, which calls for Zn-poor (Ge-rich) conditions, while Al and Ga should go on a Ge site, calling for Zn-rich (Ge-poor) conditions. Figures 2(a)-(c) also include information about other configurations of the dopant that may lead to self-compensation. The similarity in atomic size of Zn and Ge suggests that Al and Ga may choose to substitute on the Zn site instead of the Ge site, where they will act as donors. In the case of Li, self-compensation may occur by incorporation of Li as an interstitial (Li_i).

In principle we should also consider compensation by native defects. Under Zn-rich conditions, our previous calculations of defect formation energies[7] indicate that the Ge_{Zn} antisite is the lowest-energy native donor. However, its formation energy is higher than that of the Al_{Zn} and Ga_{Zn} donors, indicating that wrong-site incorporation is the more severe problem. Under Zn-poor conditions, where the incorporation of Al and Ga on the Ge-site decreases, self-compensation by Al_{Zn} and Ga_{Zn} donors remains the more severe problem. Turning to Li, under Zn-poor conditions, where the incorporation of Li_{Zn} is favored, we find compensation by the Ge_{Zn} antisite to be more severe than self-compensation. However, under Zn-rich conditions, where the formation energy of both Li_{Zn} and Ge_{Zn} is higher, we find self-compensation by Li_i to be more severe.

Li_i, Al_{Zn}, and Ga_{Zn} all act as shallow donors, i.e., the positive charge state is the only stable charge state for all Fermi-level positions. The Li interstitial is located in the octahedral site. Incorporation of Al or Ga on the Zn site leads to a symmetric relaxation of the nearest-neighbor N atoms. For Al^+_{Zn} the N atoms relax inwards by up to 6.0%, and for Ga_{Zn} by 3.4%. Al_i and Ga_i interstitials are also potential compensating donors, but we find them to have significantly higher formation energies compared to Al_{Zn} and Ga_{Zn}.

Charge neutrality requires the concentration of positively and negatively charged defects and impurities to be equal. In the absence of other defects or impurities, the presence of compensating donors pins the Fermi level at a position corresponding to the intersection point of the formation energies of the donors and acceptors. In the example of Al, the intersection between Al^+_{Zn} and Al^-_{Ge} occurs at E_F=1.63 eV; this is far away from the VBM and the material will be insulating rather than p-type.

We have also considered the formation of complexes between the negatively charged acceptors and the positively charged donors. We can assess the stability of the Al_{Ge}–Al_{Zn} and Ga_{Ge}–Ga_{Zn} complexes by calculating their formation energies. The binding energy is defined as the energy difference between the formation energy of the neutral complex (which is its only stable charge state) and the sum of the formation energies of the negative acceptor and the positive donor. The binding energies are listed in Table I.

From the results in Fig. 2 it is evident that self-

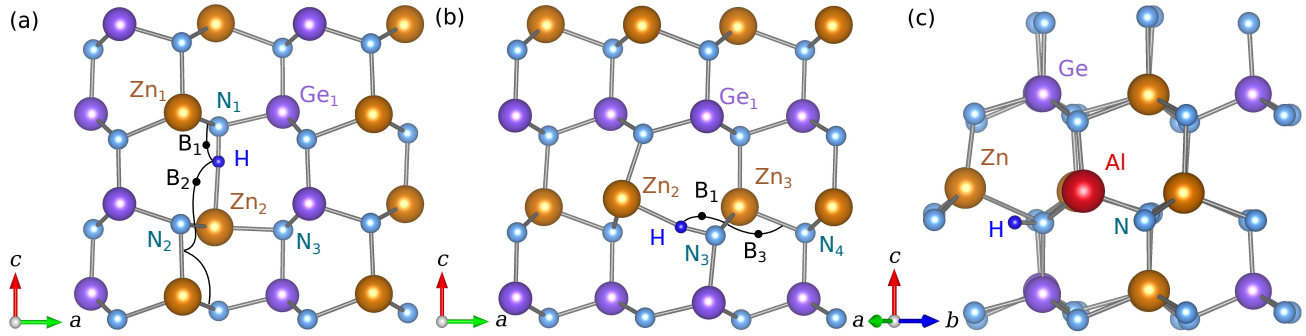

FIG. 3. (a), (b) Schematic of bonding arrangement within the two distinct layers of $ZnGeN_2$ perpendicular to the b axis, illustrating the connectivity of Zn-N bonds. (a) Path for H_i migration along the c axis, with B_1 and B_2 indicating saddle points. (b) Path for H_i migration along the a axis. A subset of atoms labeled in (a) are the same atoms as in (b). (c) Schematic illustration of the Al_{Ge}–H complex.

compensation is a serious problem. We now discuss a potential strategy to avoid or at least suppress self-compensation, namely co-doping with hydrogen. This approach is inspired by the example of Mg-doped GaN: growth in a hydrogen-rich environment (such as metal-organic chemical vapor deposition) leads to strong compensation by hydrogen donors, suppressing the incorporation of other potential compensating species in the process. However, the advantage of hydrogen as a compensating donor is that it is sufficiently mobile to be removed from the p-type layer in a post-growth anneal, leading to activation of the Mg_{Ga} acceptors.[9,27]

Figure 2 includes our calculated formation energy for interstitial H (previously reported in Ref. 7). The case of Al illustrates that the formation energy of H_i is lower than that of the compensating Al_{Zn} donor. Hydrogen will thus be preferentially incorporated, suppressing incorporation of Al on the Zn site. An additional advantage of the hydrogen co-doping is that the Fermi level where the formation energies of donors and acceptors intersect is shifted higher, leading to a decrease in the acceptor formation energy and a higher concentration of acceptors.

Still, the material that is grown in the presence of hydrogen will be completely compensated, with a Fermi level somewhere in the middle of the gap. Generating p-type material depends on the ability to remove hydrogen from the acceptor-doped layer. This needs to be accomplished at a temperature that is sufficiently high to effectively remove hydrogen, but low enough to "freeze in" the impurities at the concentrations that were established during the (hydrogen-rich) growth, and prevent formation of new defects.

To calculate migration barriers, we use the nudged elastic band (NEB) method.[28,29]In bulk $ZnGeN_2$, H_i^+ is preferentially located in a bond-center position between Zn and N. Configurations placing H_i^+ near Ge are much higher in energy; therefore, we calculate the barrier for each hop the H_i^+ ion makes between Zn-N bonds. Each hop consists of a rotation around either a N atom or a Zn atom. Net diffusion requires repeatedly making both types of hops. These hops are illustrated in Figs. 3(a) and (b), with saddle points along the hops labeled B_1, B_2, and B_3. The hop around a N atom has a low barrier of 0.2 eV. Hops around a Zn atom have a larger barrier, with a slight anisotropy: hops along the c axis [Fig. 3(a)] have a barrier of 1.3 eV, while hops along the a axis [Fig. 3(b)] have a barrier of 1.1 eV. The difference between these barriers is because the H_i^+ ion experiences slightly higher repulsion from second-nearest-neighbor Zn cations while hopping along the c axis. The hop around the N atom is much lower in energy as the H_i^+ is bonded to and remains close to the N atom throughout the hop, while the hop around the Zn atom breaks the N-H bond.

Fig. 3(a) shows a chain of Zn-N bonds along the c axis. The maximum diffusion barrier along this chain is at the saddle point B_2 with a height of 1.3 eV. Fig. 3(b) shows a chain of Zn-N bonds along the a axis. The maximum diffusion barrier along this chain is at the saddle point B_3 with a height of 1.1 eV. There is no similar chain along the b axis, but each H_i^+ ion hop has some displacement component along b. Alternating the steps illustrated for travel along the a and c axes enables net movement and diffusion along the b axis; therefore, H_i^+ can travel between Zn-N bond centers in all three spatial directions with modest migration barriers.

The H_i^+ migration barriers of 1.3 eV along the c axis and 1.1 eV along the a axis in $ZnGeN_2$ are similar to H_i^+ barriers in GaN.[30,31] This migration barrier is low enough to suggest that moving hydrogen around should not be a problem at elevated temperatures. However, H_i^+ will be attracted to the negatively charged acceptors, and thus additional energy may be required to dissociate acceptor-hydrogen complexes.

We have therefore investigated Li_{Zn}–H, Ga_{Ge}–H, and Al_{Ge}–H complexes. The Al_{Ge}–H complex is illustrated schematically in Fig. 3(c).We find each complex to be stable only in the neutral charge state. In the Li_{Zn}–H complex, hydrogen assumes a position similar to its position in the bulk, close to the center of the Li-N bond. In contrast, in the Al_{Ge}–H and Ga_{Ge}–H complexes, the H_i^+

ion sits in the antibonding position on the extension of a nearby Zn-N bond. The H_i^+ ion is not collinear with the Zn-N bond, but is shifted slightly towards the nearest Zn atom, as seen in Fig. 3(c). The binding energies for the acceptor-hydrogen complexes are listed in Table I.

We find the binding energies to be about 0.6 eV for Al and Ga; this is lower than the binding energy of the Mg–H complex in GaN, calculated to be 1.02 eV.[8] This suggests that modest annealing temperatures can be used to disassociate such complexes and remove the hydrogen. As illustrated by Fig. 2 and Table I, Al appears to be the best candidate for *p*-type doping of $ZnGeN_2$.

We note that the formation energies in Fig. 2 are plotted for specific choices of the chemical potentials. Specifically, we assumed the highest possible chemical potential of the impurity, corresponding to the solubility limit. At lower impurity concentrations the extent to which hydrogen suppresses compensation would be stronger. In addition, growth conditions that are more hydrogen-rich than assumed in Fig. 2 may be achievable.

In summary, using first-principles calculations we have determined the acceptor ionization energies for a wide range of candidate dopants in $ZnGeN_2$. The ionization energy of Al_{Ge} is only 0.24 eV, which is comparable to Mg in GaN. We proposed co-doping with hydrogen as a strategy to surmount issues of compensation: incorporation of hydrogen suppresses the formation of self-compensating donors, and hydrogen can be removed in a post-growth anneal.

This work was supported by the Army Research Office (W911NF-16-1-0538). Work by D. W. was supported by the U. S. Department of Energy (DOE), Office of Science, Basic Energy Sciences (BES) under Award No. DE-SC0010689. Computational resources were provided by the Extreme Science and Engineering Discovery Environment (XSEDE), which is supported by National Science Foundation grant number ACI-1548562, the Department of Defense High Performance Computing Modernization Program at the Army Research Office/Office of Naval Research (Project No. ARONC4175) and the Center for Scientific Computing from the CNSI, MRL: an NSF MRSEC (DMR-1720256) and NSF CNS-1725797.

[1] T. Misaki, A. Wakahara, H. Okada, and A. Yoshida, J. Cryst. Growth **260**, 125 (2004).
[2] S. Kikkawa and H. Morisaka, Solid State Communications **112**, 513 (1999).
[3] L. Han, C. Lieberman, and H. Zhao, J. Appl. Phys. **121**, 093101 (2017).
[4] A. D. Martinez, A. N. Fioretti, E. S. Toberer, and A. C. Tamboli, J. Mater. Chem. A , (2017).
[5] L. Han, K. Kash, and H. Zhao, J. Appl. Phys. **120**, 103102 (2016).
[6] J. S. Dyck, J. R. Colvin, P. C. Quayle, T. J. Peshek, and K. Kash, Journal of Electronic Materials **45**, 2920 (2016).
[7] N. L. Adamski, Z. Zhu, D. Wickramaratne, and C. G. V. de Walle, J. Appl. Phys. **122**, 195701 (2017).
[8] J. L. Lyons, A. Janotti, and C. G. Van de Walle, Phys. Rev. Lett. **108**, 156403 (2012).
[9] S. Nakamura, T. Mukai, M. Senoh, and N. Iwasa, Jpn. J. Appl. Phys. **31**, L139 (1992).
[10] D. Skachkov, A. Punya Jaroenjittichai, L.-y. Huang, and W. R. L. Lambrecht, Phys. Rev. B **93**, 155202 (2016).
[11] C. Freysoldt, B. Grabowski, T. Hickel, J. Neugebauer, G. Kresse, A. Janotti, and C. G. Van de Walle, Rev. Mod. Phys. **86**, 253 (2014).
[12] J. L. Lyons, A. Janotti, and C. G. V. de Walle, J. Appl. Phys. **115**, 012014 (2014).
[13] T. Wang, C. Ni, and A. Janotti, Phys. Rev. B **95**, 205205 (2017).
[14] P. Blöchl, Phys. Rev. B **50**, 17953 (1994).
[15] G. Kresse and J. Hafner, Phys. Rev. B **47**, 558 (1993).
[16] G. Kresse and J. Furthmüller, Comput. Mater. Sci. **6**, 15 (1996).
[17] J. Heyd, G. E. Scuseria, and M. Ernzerhof, J. Chem. Phys. **118**, 8207 (2003).
[18] J. Heyd, G. E. Scuseria, and M. Ernzerhof, J. Chem. Phys. **124**, 219906 (2006).
[19] M. Wintenberger, M. Maunaye, and Y. Laurent, Materials Research Bulletin **8**, 1049 (1973).
[20] P. C. Quayle, E. W. Blanton, A. Punya, G. T. Junno, K. He, L. Han, H. Zhao, J. Shan, W. R. L. Lambrecht, and K. Kash, Phys. Rev. B **91**, 205207 (2015).
[21] A. Punya, W. R. L. Lambrecht, and M. van Schilfgaarde, Phys. Rev. B **84**, 165204 (2011).
[22] C. Freysoldt, J. Neugebauer, and C. G. Van de Walle, Phys. Rev. Lett. **102**, 016402 (2009).
[23] C. Freysoldt, J. Neugebauer, and C. G. Van de Walle, Phys. Status Solidi B **248**, 1067 (2011).
[24] O. Madelung, *Semiconductors-Basic Data, 2nd revised ed.* (Springer, Berlin, 1996).
[25] P. O'Hare and G. K. Johnson, J. Chem. Thermodyn. **7**, 13 (1975).
[26] R. D. Shannon, Acta Cryst. **A32**, 751,767 (1976).
[27] J. Neugebauer and C. G. Van de Walle, Phys. Rev. Lett. **75**, 4452 (1995).
[28] G. Henkelman, B. P. Uberuaga, and H. Jónsson, J. Chem. Phys. **113**, 9901 (2000).
[29] G. Henkelman and H. Jónsson, J. Chem. Phys. **113**, 9978 (2000).
[30] J.-S. Park and K. J. Chang, Appl. Phys. Express **5**, 065601 (2012).
[31] C. H. Seager, S. M. Myers, A. F. Wright, D. D. Koleske, and A. A. Allerman, J. Appl. Phys. **92**, 7246 (2002).